Flapping-wing flight in bird-sized uavs for the robur project: from an evolutionary optimization to a real flapping-wing mechanism

Emmanuel De Margerie, Jean-Baptiste Mouret, Stéphane Doncieux, Jean-Arcady Meyer, Thomas Ravasi, Pascal Martinelli, Christophe Grand

3rd US-European Competition and Workshop on Micro Air Vehicle Systems (MAV07) & European Micro Air Vehicle Conference and Flight Competition (EMAV2007), 17-21 September 2007, Toulouse, France

Flapping-wing flight in bird-sized UAVs for the ROBUR project: from an evolutionary optimization to a real flapping-wing mechanism

Emmanuel de Margerie[*], Jean-Baptiste Mouret[†]
Stéphane Doncieux[‡], Jean-Arcady Meyer[§]
ISIR, Institut des Systèmes Intelligents et Robotique
LIP6, 104, avenue du Président Kennedy 75016 Paris, FRANCE

Thomas Ravasi[¶], Pascal Martinelli[‖], Christophe Grand[**]
Institut Universitaire de Technologie de Cachan
9 avenue de la division Leclerc 94230 Cachan, FRANCE

Birds daily execute complex maneuvers out of reach for current UAVs of comparable size, and these capacities are a least partly linked to efficient flapping kinematics. This article describes research efforts contributing to the ROBUR project that aims at producing a bird-sized UAV relying on such advanced kinematics.

First, a multi-objective evolutionary algorithm was used to provide insights about the range of key mechanical parameters required for a 0.5 kg UAV flying horizontally at different speeds. Optimization lead to a minimum energy consumption of 20-50 W/kg for a 10-12 m/s speed, with wing-beat frequencies between 3 to 5 Hz. The corresponding simulations indicate that wing folding would substantially decrease the power consumption (25-44%) at medium to high speeds. Then, these results guided the design of a parallel flapping-wing mechanism based on two connected rod-crank devices. Wing motion is produced by four position-controlled brushless motors and the corresponding kinematic model is described in this article. Wing folding mechanism design will be the subject of future work.

I. Introduction

THe capabilities of mini-UAVs have drastically increased thanks to recent advances in terms of energy storage, effector power and electronic miniaturization, but they still remain far below the maneuverability and energy efficiency exhibited by birds and bats. An European kestrel for instance can remain above an interesting objective, fly forward at varying speeds, glide or soar to save energy, while demonstrating maneuverability capacities that far exceed those of the most efficient acrobatic aircrafts. Although they may also display impressive flying aptitudes, insects are less interesting in an UAV perspective because their limited payload restricts their applicability to indoor flight and to situations that can be dealt with few sensors or short computational power. For this reason, we have chosen to study flapping-flight for bird-sized UAVs, i.e., with a wing-span ranging from 0.5 to 1 meter and a weight of 500 g.

This article describes current research efforts targeted at designing a flapping-wing platform within the ROBUR project.[1] Whereas current flapping-flight artifacts show a maneuverability similar to that of fixed-wing engines, our overall objective is to design an aircraft whose capabilities will more closely resemble that of a kestrel, or at least of a pigeon. To this end, the wing kinematics have to be carefully

[*]Post-doc, dept SIMA, Emmanuel.De-margerie@lip6.fr
[†]Ph.D. Student, dept SIMA, Jean-Baptiste.Mouret@lip6.fr
[‡]Prof. assistant, dept SIMA, Stephane.Doncieux@upmc.fr
[§]Emeritus Research Director, dept SIMA, Jean-Arcady.Meyer@lip6.fr
[¶]Student, IUT de Cachan
[‖]Prof. assistant, IUT de Cachan, Pascal.martinelli@u-psud.fr
[**]Prof. assistant, IUT de Cachan, grand@robot.jussieu.fr

controlled, for instance through the implementation of a neural network-based closed-loop control.[1] As a consequence, the mechanical instantiation of our artificial bird must be able to move its wings on a wide range of periodical and non periodical trajectories, while remaining as energy-efficient as possible. This makes the corresponding wing-beat mechanism different from many realizations described in the literature[2–5] or exploited by hobbyists[a], because they generate periodical or quasi-sinusoidal movements only. The design of such an improved device is especially challenging since, to properly size its actuators and mechanical parts, we must know the order of magnitude of torques, angle ranges and dimensions, which strongly depend on the wing-beat kinematics and on the morphology of the artificial bird. The optimal kinematics, the necessary degrees of freedom, and the required power to fly at a given speed still being open scientific questions, we want to address them while designing such a flapping-wing device.

Our overall strategy to tackle this chicken-and-egg issue may be decomposed in at least four stages. In the first one, simulations will serve to compare different morphologies and kinematics adapted to various flying speeds. The second stage will be devoted to the design of a mechanism able to efficiently flap two wings for straight-line flight. The implementation and adaptation of this device on a real platform will be the objective of the third stage. Finally, more complex maneuvers could be at the core of the fourth and subsequent stages.

This article describes results obtained so far, which complete the first two stages.

II. Evolutionary optimization

II.A. Search space and evolutionary algorithm

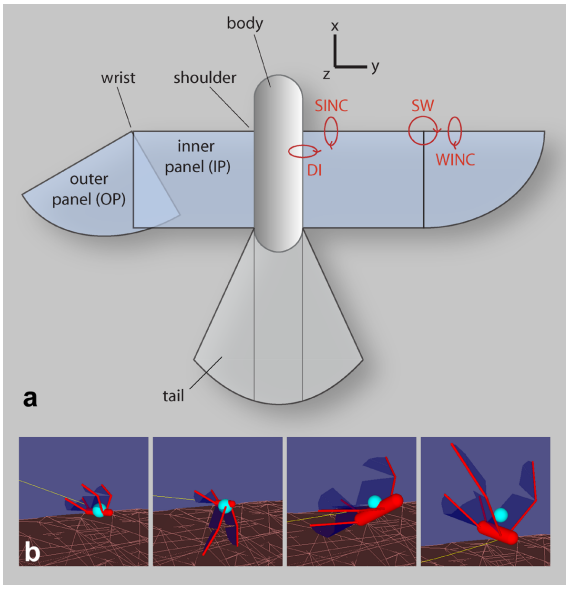

Figure 1. The morphology of a simulated UAV. a: Wing panels and their DOFs (dihedral (DI), sweep (SW), shoulder incidence (SINC) and wrist incidence (WINC)). b: Possible morphologies corresponding to boundary values of wing area (0.1-0.4 m2) and wing aspect ratio (4.5-10).

To specify the range of key mechanical parameters required for making horizontal flight at different speeds possible, an optimization procedure was applied to a generic bird-inspired morphological structure, with wings articulated at the joint with the UAV body (shoulder) and at mid-span (wrist). Thus, the wrist joined an inner and an outer wing panels, contributing to the articulated character of the UAV's wing (Fig. 1). Both panels were considered as non-deformable surfaces with high-lift and low-Reynolds numbers (Selig 4083). Wing movements depended upon an open-loop controller applying a sinusoidal pattern at 4 angular DOFs: the dihedral and incidence angles at the shoulder, the sweep and incidence angles at the wrist (the wrist sweep allowed the outer wing panel to be partially and temporarily retracted during the flapping stroke, Fig. 1). Each individual's body weighted 0.5 kg, plus the mass of wings and tail, which isometrically depended on their respective areas (the tail area was constrained to be half the area of the wing).

The morphological parameters to be optimized were the wing area (in the range 0.1-0.4 m2) and the wing aspect ratio (in the range 4.5 - 10). Likewise, the kinematic parameters that were optimized were the flapping frequency (in the range 1-10 Hz, common to all DOFs), the amplitude of rotation for each DOF, an offset for each panel's twist angle, and the time offsets between the dihedral and every other DOF. The corresponding ranges were selected according to biological data characterizing birds with a similar mass.[6,7] As a whole, the optimization procedure worked on 12 floating point parameters to seek an efficient flapping stroke.

The fitness of each individual generated was tested in a specific flight simulator, based on steady aerody-

[a] http://www.ornithopter.org

namics and taking wing aspect ratios and Reynolds numbers into account. This semi-empirical panel-based simulator generated realistic variations of the lift and drag components whatever the local direction of free stream velocity was. It has been calibrated and partially validated using experimental lift and drag curves of the Selig 4083 airfoil and wind-tunnel measurements.[8]

Two objectives were optimized simultaneously: the best UAVs were those that flew along the most horizontal path, for at least 10 s., and with the lowest mechanical power. The latter characteristic was evaluated through torques produced at joints and relied on the assumption that the costs to slow down or accelerate the rotation of a joint were equivalent, assuming that a real UAV would not use an elastic energy storage capacity.

The $\varepsilon - MOGA$[9] multi-objective evolutionary algorithm was used to simultaneously optimize these two objectives. The corresponding approach relies on the *domination* concept. A solution $\mathbf{x}^{(1)}$ is said to dominate another solution $\mathbf{x}^{(2)}$ if and only if:

- the solution $\mathbf{x}^{(1)}$ is not worse than $\mathbf{x}^{(2)}$ with respect to all objectives;
- the solution $\mathbf{x}^{(1)}$ is strictly better than $\mathbf{x}^{(2)}$ with respect to at least one objective.

An individual is said to be *Pareto-optimal* if it is not dominated. In contrast to traditional evolutionary algorithms, $\varepsilon - MOGA$ produces a set of non-dominated individuals instead of a single solution, each of these individuals representing an optimal trade-off between the optimized objectives.

A total of 24 evolutionary runs were performed, for target horizontal speeds ranging from 6 to 20 m/s.

II.B. Results

Results showed that power levels for achieving steady horizontal flight were minimal at medium speeds (10-12 m/s), attaining 20 W per kg of UAV mass (Fig. 2a). To fly at higher speeds (16-20 m/s), mechanical power increased to 30-50 W/kg for the best individuals. Flight at lower speed was possible, but power increased dramatically, up to 500 W/kg at 6 m/s. Although 20-50 W/kg power appeared satisfactory, approaching in-vivo data in birds,[10,11] unrealistic high power levels obtained at low speed probably reflected some limitations of our simulator, which did not take unsteady aerodynamic effects into account, and/or of the sinusoidal kinematics, simpler than those used by birds.

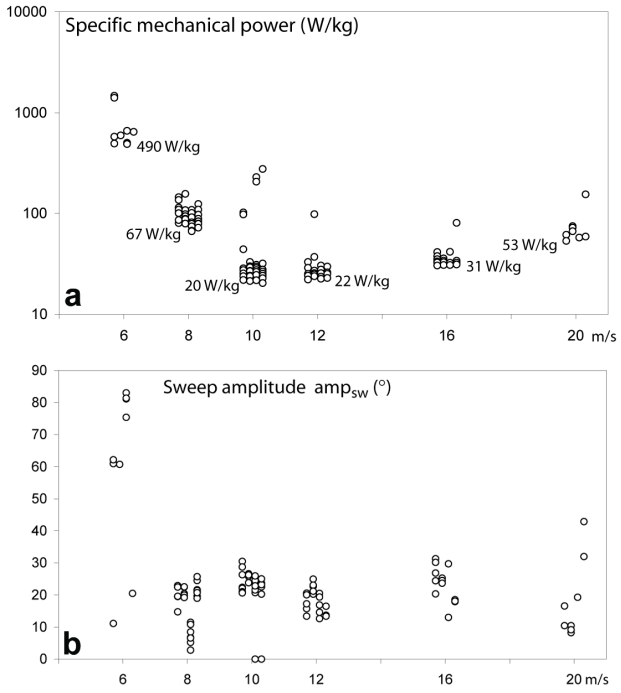

Figure 2. Morpho-kinematic adaptations to different flight speeds. Characters of the best individuals obtained in 4 evolutionary runs for 6 flight speeds (6, 8, 10, 12, 16 and 20 m/s) are aligned vertically. a: Specific mechanical power consumption; b: Amplitude of wrist sweep angular oscillation during the flapping stroke.

Morphological adaptation to different flight speed mainly implied a reduction of wing area (hence an increase of wing loading) at higher speed. Wing aspect ratio converged to high values (approx. 10) at all flying speeds, probably reflecting the fact that we only selected morphologies for forward flight and put no selective pressure on maneuverability for example. Kinematic adaptations resulted in minimal flapping frequencies (near 3 Hz) at medium speed, increasing to approx. 5 Hz at both low and high speeds. At low speed, incidence variation of wing panels throughout the flapping stroke significantly increased (attaining +/- 20 degrees or more for the outer wing panel), and the UAV's body tended to adopt a strongly "head up" tilted position, as has been reported in birds.[12] An analysis of aerodynamic forces on wing panels at each flying speed showed that, generally, the wing outer panel was almost inactive

during upstroke, while it produced lift and thrust forces during the down-stroke. The inner panel tended to produce lift forces during both downstrokes and upstrokes, but no thrust forces, except at the highest flying speeds.

Most interesting were the results concerning the wrist (Fig. 2b). Wrist sweep was used by evolution at all flying speeds: the sweep amplitude attained 60 degrees and more at 6 m/s, while it averaged 25 at other speeds. At 6 m/s, its role was clearly to decelerate the wing tip during upstroke, and to accelerate it during downstroke. At higher speeds, the aerodynamic role of the wrist sweep was less straightforward, but supplementary evolution runs without this DOF (i.e. with wings reduced to a single panel) showed that the use of sweep was responsible for a 25-44% decrease in power consumption at medium speed, and for a 7-17% decrease at high speed. These results strongly suggest that the design of articulated rigid wings for flapping-wing UAVs may really be worth the technical cost of an additional controlled joint, if one considers in-flight power saving.

Speed (m/s)	Dihedral	Shoulder incidence	Wrist incidence
6-8	15-50	0-30	10-50
10-12	25-45	0-15	8-15
16-20	30-65	0-5	1-10

Figure 3. Angular ranges (in degrees) for three DOFs (wing folding is not represented) for Pareto-optimal individuals.

In the perspective of designing a flapping mechanism, the following conclusions could be drawn from the optimization results thus obtained:

- Minimal power was attained at 10-12 m/s, which could be our targeted speed.
- Lower speeds seem unattainable given the morphology used, the sinusoidal kinematics and the aerodynamic effects taken in account in the simulator. Additional research efforts should be devoted to better understand slow speed kinematics and aerodynamics.
- Wings with high aspect ratio (10) seem well adapted to forward flight. Additional studies would be required to explore their maneuverability capacities.
- Power required to fly at 10-12 m/s was at least 20 W/kg.
- Wing folding substantially decreased the power consumption (25-44%).
- Typical flapping frequencies were in the range 3-5 Hz.
- Figure 3 shows the angle ranges obtained for the different DOFs, with Pareto-optimal kinematics. This means that at least similar ranges should be afforded to the DOFs of our future UAV to make basic straight-line flight possible.

III. Mechanical design

Capitalizing on these results, we designed a wing-beating mechanism that allows a wide range of dihedral and twist variations, with a high energetic and mechanical efficiency. To reach such capabilities, an innovative mechanism was developed[b] as shown in figure 4. Wing folding won't be considered here, it will be the subject of future work.

In this mechanism, wing motions are produced by four position-controlled brushless motors (each motor is about 30W power and 100g weight). These four motors are associated two by two, constituting a parallel mechanism that uses two connected rod-crank devices. Thus, the wings can be moved to follow an arbitrary trajectory and the power required to execute the quasi-sinusoidal movements is especially low. Each pair of motors is used to respectively control: (1) the dihedral (DI) motion and (2) the shoulder incidence (SINC) motion.

[b]Within the CRIC, an institution related to the IUT Cachan

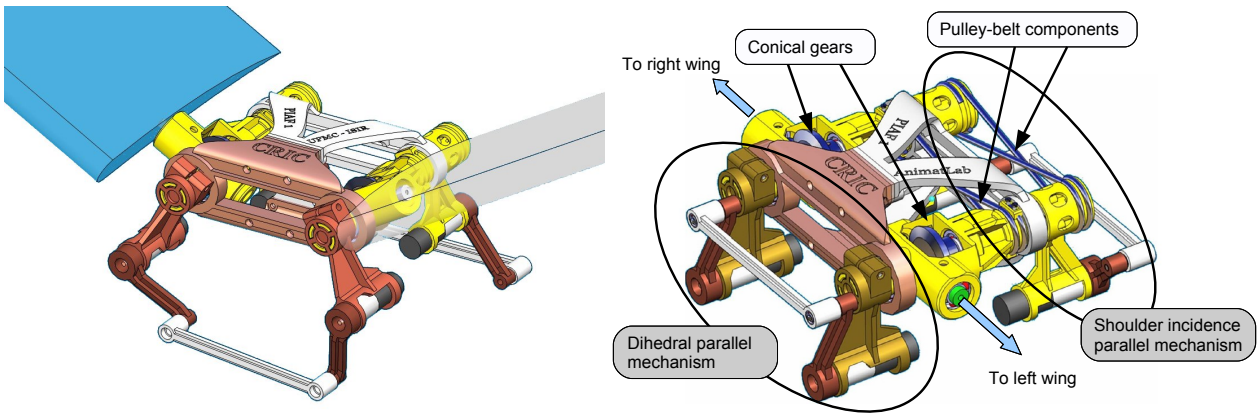

(a) General view

(b) Detailed view with sub-components

Figure 4. Wing-beating mechanism.

III.A. Kinematical modeling

The wing-beating system is composed of two identical mechanisms. Each one is a parallel system actuated by two motors. The first one, located in the front plane, is directly used to control the dihedral motion of the wings and the second one, located on the rear plane, controls the shoulder incidence motion through two conical gears. Each of these elementary systems is made symmetrical by using a drive-belt component (see figure 4). Thus, in this prototype, the flapping motion is identical for left and right wings (both for dihedral and twist motion).

The elementary parallel mechanism is composed of five rods connected through six revolute joints. The figure 5 shows the kinematic schema of this parallel mechanism. Joint J_1 and J_2 are coupled by the drive-belt, joint J_3 and J_4 are actuated by two motors, and the last two joints (J_5, J_6) remain free. The mobility index of the mechanism is given by the classical Grubler equation :

$$m = \sum_{i=1}^{n} f_i - 3(n-b)$$

where b is the number of moving bodies, n the number of joints, f_i the number of degrees of freedom of each joint i. In this case, the mobility index is $m = 3$ (5 bodies, 6 revolute joints), but the overall system mobility is reduced to $m = 2$ when the symmetry condition from the drive-belt is considered. As these two degrees of freedom are actuated by two motors, the corresponding motion is completely constrained.

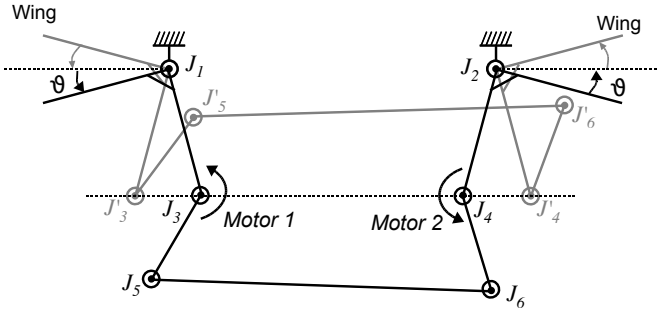

Figure 5. Kinematic schema of the parallel mechanism

For analysis purpose, the system can be simplified by the kinematically equivalent system depicted in figure 6(b). Because of the symmetrical constraint on joints J_1 and J_2 (angle θ), the motion of points A_3

and A_4 is constrained to an horizontal axis (A_i denotes the center of joint J_i). Thus, we can consider the 3-rod mechanism only, and express the kinematic relation between λ and the input angles α_1 and α_2. The solution is obtained by solving the kinematical closure-form equations :

$$\begin{cases} b\cos\alpha_1 + L\cos\gamma - b\cos\alpha_2 = \lambda \\ b\sin\alpha_1 + L\sin\gamma - b\sin\alpha_2 = 0 \end{cases} \tag{1}$$

Eliminating γ from these equations gives the following expression:

$$L^2 = \big(\lambda + b(\cos\alpha_1 - \cos\alpha_2)\big)^2 + b^2(\sin\alpha_1 - \sin\alpha_2)^2 \tag{2}$$

Then, λ can be determined from this second order equation. When the solution existing condition is satisfied ($L > \sqrt{2}b$), we obtain the following unique solution:

$$\lambda = \sqrt{L^2 - b^2(\sin\alpha_1 - \sin\alpha_2)^2} + b(\cos\alpha_1 - \cos\alpha_2) \tag{3}$$

And, considering the schema on figure 6(a), the wing flapping angle ϑ is given as a function of λ:

$$\vartheta = \sin^{-1}\frac{L-\lambda}{2a} \tag{4}$$

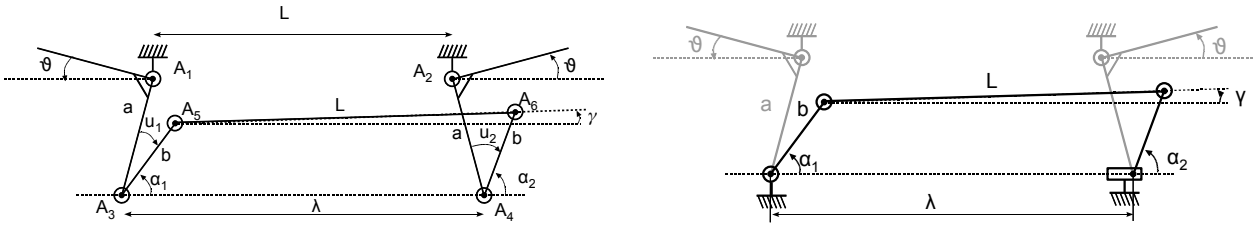

(a) Kinematical parameters (b) Simplified schema

Figure 6. Detailed kinematic schema

It should be noticed that the parameters α_1 and α_2 are not directly the control inputs. But, we can instead consider $\mathbf{u} = [u_1\ u_2]^t$ the input vector composed of the two motor angles (corresponding to the joint angles of J_3 and J_4), that can be computed as function of the parameters α_1, α_2 and the kinematical configuration of the mechanism characterized by the angle ϑ:

$$\begin{cases} u_1 = (\alpha_1 - \frac{\pi}{2}) - \vartheta \\ u_2 = (\alpha_2 - \frac{\pi}{2}) + \vartheta \end{cases}$$

However for the mathematical description of the kinematical model, it is more efficient to consider the input parameters α_1 and α_2 instead of the motor angles u_1 and u_2, we will consequently use α_1 and α_2 to further describe the model.

III.B. Model reduction

The system presents two control inputs α_1 and α_2 for one state parameter ϑ. Therefore, the mechanism is over-actuated and we need to determine compatible angles. We introduce a new set of input variables α and φ, respectively the mean input angle and the half-phase angle :

$$\begin{cases} \alpha = \frac{1}{2}(\alpha_2 + \alpha_1) \\ \varphi = \frac{1}{2}(\alpha_2 - \alpha_1) \end{cases} \quad \text{and} \quad \begin{cases} \alpha_1 = \alpha - \varphi \\ \alpha_2 = \alpha + \varphi \end{cases}$$

Such as equation (3) becomes:

$$\lambda = \sqrt{L^2 - 4b^2 \cos^2\alpha \, \sin^2\varphi} + 2b \, \sin\alpha \, \sin\varphi \tag{5}$$

Likewise, the relations between the motor angular positions (u_1 and u_2) and the new variables become:

$$\begin{cases} u_1 = (\alpha - \frac{\pi}{2}) - (\vartheta + \varphi) \\ u_2 = (\alpha - \frac{\pi}{2}) + (\vartheta + \varphi) \end{cases} \quad \text{and} \quad \begin{cases} \alpha &= \frac{1}{2}(u_2 + u_1) + \frac{\pi}{2} \\ \varphi + \vartheta &= \frac{1}{2}(u_2 - u_1) \end{cases}$$

III.C. Sinusoidal motion control of the flapping angle

The consideration of variables α and φ leads to a simplified control model of the wing-flapping motion. Indeed, it allows to define a quasi-sinusoidal motion securing the desired flapping frequency and amplitude.

Equation (5) can be differentiated with respect to α:

$$\frac{d\lambda}{d\alpha} = 2b \cos\alpha \, \sin\varphi \left[1 + \frac{2b \sin\alpha \, \sin\varphi}{\sqrt{\frac{L^2}{4b^2} - cos^2\alpha \, \sin^2\varphi}} \right] \tag{6}$$

Considering the schema depicted in figure 5, one can conclude that the wing angle ϑ is extreme when λ is also extreme. In order to find the extreme positions $\alpha_{\min}$ and $\alpha_{\max}$, the relation $\frac{d\lambda}{d\alpha} = 0$ must be solved. This leads to the following solutions:

$$\begin{cases} \cos\alpha = 0 \\ \sin\varphi = \pm\frac{L}{2b} \end{cases} \tag{7}$$

Thus, for any values of φ, there are only two extreme positions at each periode that are solutions of $\cos\alpha = 0$. Introducing this result in equations (5) and (4), we can find the maximum values for λ and consequently for ϑ :

$$\begin{cases} \lambda_{\max} = L \pm 2\,b \, \sin\varphi \\ a \sin\vartheta_{\max} = b \sin\varphi \end{cases} \tag{8}$$

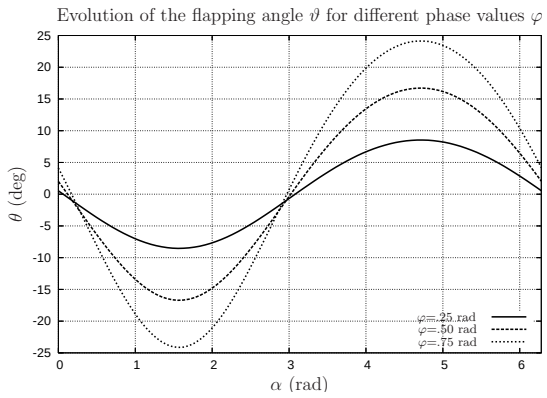

Figure 7. Exemple of ϑ trajectory obtained with kinematic based control

Figure 7 shows some trajectories ϑ obtained for different phase angles φ. The motion is quasi-sinusoidal, its amplitude depends on φ and its frequency can be modulated thanks to the velocity term $\dot{\alpha}$. Therefore, if the desired quasi-sinusoidal trajectory is specified by its frequency f_ϑ and its amplitude $\vartheta_{\max}$, the velocity $\dot{\alpha}$ and the phase are determined as follow:

$$\begin{cases} \dot{\alpha} = 2\pi f_\vartheta \\ \varphi = \sin^{-1}\left(\frac{a}{b}\sin\vartheta_{\max}\right) \end{cases} \tag{9}$$

III.D. Pseudo-periodical motion controller

In order to extent this simple quasi-sinusoidal control to an arbitrary flapping motion, we need to investigate the differential kinematic model. The flapping velocity is given by $\dot{\vartheta}$ that can be expressed as a fonction of the input velocities ($\dot{\alpha}$, $\dot{\varphi}$):

$$\dot{\vartheta} \;=\; \frac{d\vartheta}{d\lambda}\left(\frac{d\lambda}{d\alpha}\dot{\alpha} + \frac{d\lambda}{d\varphi}\dot{\varphi}\right) = J_\alpha\dot{\alpha} + J_\varphi\dot{\varphi} \tag{10}$$

The corresponding jacobian terms are determined from equations (4) and (6):

$$\begin{cases} J_\alpha = \frac{d\vartheta}{d\lambda}\frac{d\lambda}{d\alpha} = -\frac{b\cos\alpha \, \sin\varphi}{a\sqrt{1-\left(\frac{L-\lambda}{2a}\right)^2}} \left[1 + \frac{2b\sin\alpha \, \sin\varphi}{\sqrt{\frac{L^2}{4b^2} - cos^2\alpha \, \sin^2\varphi}} \right] \\ J_\varphi = \frac{d\vartheta}{d\lambda}\frac{d\lambda}{d\varphi} = -\frac{b\sin\alpha \, \cos\varphi}{a\sqrt{1-\left(\frac{L-\lambda}{2a}\right)^2}} \left[1 - \frac{2b\cos\alpha \, \cot\alpha\sin\varphi}{\sqrt{\frac{L^2}{4b^2} - cos^2\alpha \, \sin^2\varphi}} \right] \end{cases} \tag{11}$$

Then, the control principle is to compute the instantaneous velocity terms ($\dot{\alpha}$, $\dot{\varphi}$) as a function of the desired flapping velocity $\dot{\vartheta}^c$. This desired velocity becomes the control input used to follow a desired trajectory $\vartheta(t)$ with a classical feedforward controller:

$$\dot{\vartheta}^c = K_1(\vartheta - \vartheta^m) + \dot{\vartheta} \tag{12}$$

where ϑ^m is the mesured flapping velocity, K_1 is a positive gain and $\dot{\vartheta}$ is the feedforward velocity computed from the trajectory $\vartheta(t)$. Then, the control law becomes:

$$\begin{cases} \dot{\varphi} = K_2(\varphi^d - \varphi^m) \\ \dot{\alpha} = \dfrac{1}{J_\alpha}\left(\dot{\vartheta}^c - J_\varphi \dot{\varphi}\right) \end{cases} \tag{13}$$

where φ^d is the phase angle determined from the maximum absolute values of the flapping angle trajectory $\vartheta(t)$ on a given time horizon.

IV. Conclusion

These results constitute the first stepping-stones towards the generation of a fully maneuverable flapping-wing UAV. The horizontal flight of a bird-inspired UAV - with rigid wings articulated at the joint with the UAV body and at mid-span - has been simulated. Using a multi-objective evolutionary procedure, we were able to determine, at realistic typical flight speeds (10-12 m/s), the required angular ranges for the degrees of freedom, the flapping frequencies and orders of magnitude of required power to fly at different speed with simplified kinematics (20-30 W/kg). These data are consistent with zoological records for medium to high speed. Moreover, the simulations highlighted the energetic gain of wing folding for medium to high speed flights.

The corresponding results have been used to properly dimension a Flapping mechanism able to move the wing dihedral and incidence in order to follow arbitrary kinematics. The kinematic model of this innovative parallel mechanism has been detailed in this paper. Based on this model, a simple control law for quasi-sinusoidal motions has been developed. Its extension to a velocity model based controller that is able to follow various cyclic trajectories has been proposed.

The next step along the whole ROBUR project will consist in validating the model, the mechanism and the control laws described herein through wind-tunnel experiments and basic aerodynamic measurements such as the lift and drag forces thus produced. This would allow us to quantify the real energy consumption for different kinematics and to improve the simulation model, hopefully leading to an improved mechanism that would be implemented in a real UAV.

V. Acknowledgements

This study benefited from a grant from PARINOV comittee. Emmanuel de Margerie had a post-doctoral grant from DGA.

References

[1]Doncieux, S., Mouret, J.-B., Angeli, A., Barate, R., Meyer, J.-A., and de Margerie, E., "Building an Artificial Bird: Goals and Accomplishments of the ROBUR Project," *European Micro Aerial Vehicles (EMAV)*, 2006.

[2]Pornsin-Sirirak, T., Tai, Y., Ho, C., and Keennon, M., "Microbat: A Palm-Sized Electrically Powered Ornithopter," *Proceedings of NASA/JPL Workshop on Biomorphic Robotics*, 2001.

[3]Vest, M. S. and Katz, J., "Aerodynamic Study of a Flapping-Wing Micro-UAV," *37th AIAA Aerospace Sciences Meeting and Exhibit*, 1999.

[4]Raney, D. and Slominski, E., "Mechanization and Control Concepts for Biologically Inspired Micro Air Vehicles," *Journal of Aircraft*, Vol. 41, No. 6, 2004, pp. 1257–1265.

[5]Hunt, R., Hornby, G., and Lohn, J., "Toward evolved flight," *Proceedings of the 2005 conference on Genetic and evolutionary computation*, 2005, pp. 957–964.

[6]Greenewalt, C., "Dimensional relationship for flying animals," *Smithsonian Miscellaneous Collections*, Vol. 144, 1962.

[7]Norberg, U. M., *Vertebrate Flight*, Springer-Verlag, 1990.

[8]Druot, T., "Static validation of the ornithopter aerodynamic model," Tech. rep., Ensica / Université Paul Sabatier, 2004.

[9]K. Deb, M. Mohan, S. M., "Evaluating the ε-Domination Based Multi-Objective Evolutionary Algorithm for a Quick Computation of Pareto-Optimal Solutions," *Evolutionary Computation*, Vol. 13, No. 4, Winter 2005, pp. 501–525.

[10]Dial, K. P., Biewener, A. A., Tobalske, B. W., and Warrick, D. R., "Mechanical power output of bird flight," *Nature*, Vol. 390, No. 6655, 1997, pp. 67–70.

[11]Tobalske, B. W., Hedrick, T. L., Dial, K. P., and Biewener, A. A., "Comparative power curves in bird flight," *Nature*, Vol. 421, No. 6921, 2003, pp. 363–366.

[12]Tobalske, B. W. and Dial, K. P., "Flight Kinematics of black-billed magpies and pigeons over a wide range of speeds," *Journal of Experimental Biology*, Vol. 199, 1996, pp. 263–280.